Nano Today 46 (2022) 101605

Contents lists available at ScienceDirect

Nano Today

journal homepage: www.elsevier.com/locate/nanotoday

Sunlight-induced tri-state spin memory in photovoltaic/ferromagnetic heterostructure

Yifan Zhao[a,d,1], Yujing Du[a,d,1], Lei Wang[b,*], Kai Chen[c], Zhenlin Luo[c], Wensheng Yan[c], Qian Li[c,*], Zhuangde Jiang[d], Ming Liu[a,d], Ziyao Zhou[a,d,**]

[a] Electronic Materials Research Laboratory, Key Laboratory of the Ministry of Education & International Center for Dielectric Research, School of Electronic Science and Engineering, the International Joint Laboratory for Micro/Nano Manufacturing and Measurement Technology, Xi'an Jiaotong University, Xi'an 710049, China
[b] Center for Spintronics and Quantum Systems, State Key Laboratory for Mechanical Behavior of Materials, Xi'an Jiaotong University, No.28 Xianning West Road, Xi'an, Shaanxi 710049, China
[c] National Synchrotron Radiation Laboratory, University of Science and Technology of China, Hefei, Anhui 230029, China
[d] State Key Laboratory for Manufacturing Systems Engineering, Collaborative Innovation Center of High-End Manufacturing Equipment, the International Joint Laboratory for Micro/Nano Manufacturing and Measurement Technology, Xi'an Jiaotong University, Xi'an 710049, China

ARTICLE INFO

Article history:
Received 29 November 2021
Received in revised form 3 July 2022
Accepted 28 August 2022
Available online 13 September 2022

Keywords:
Interfacial magnetism
Optical-magneto-electric coupling
Photovoltaic control
Non-volatility

ABSTRACT

The advanced spintronic devices demand a new routine of manipulating spin states effectively with low power consumption, fast switching, and non-volatility. Here, a photovoltaic heterojunction structure of (Cu, Ta)/$Co_{40}Fe_{40}B_{20}$/(Ta, Cu) on a p-n junction Si wafer is proposed. The saturation magnetizations (M_s) tunability under sunlight illumination is decreased by ~5–8 %. The first principle calculations reveal that the insert Cu or Ta layer promoted the photoelectron transmission, leading to a larger M_s tunability. Moreover, the Ta layer also generates a barrier between the p-n junction and CoFeB to keep the photoelectrons in the CoFeB layer, creating a non-volatility and sunlight/electrical dual-regulated tri-state magnetization change. Element-resolved X-ray magnetic circular dichroism (XMCD) measurement is also performed to determine the diminished intrinsic magnetism and corresponding non-volatility during sunlight illumination. These fundings explore a new method of magnetic modulation further to expand the non-volatile, low-power sunlight-driven spintronics.

Introduction

Spintronics play a key role in memory and logic applications. The spintronic application is usually energy-efficient compared with electronic devices because alternating spin states are easier than moving electrons.[1–9] The increasing demand for pursuing energy-saving and high-efficient spintronic devices drives researchers to improve spin-manipulation methods. Traditionally, spins are tuned by the magnetic field; however, realizing localized magnetic fields requires bulky, energy-inefficient, noisy, vulnerable magnetic heads. [10–13] The spin-polarized current, easily incorporated in integrated circuits, is also developed to regulate the spin condition.[1,14–17] Nevertheless, the current-driven spintronics still suffer from Joule-heating problems, leading to high energy consumption, small storage density, and limited processing speed.[18,19] In the recent decade, voltage control of magnetism in ferromagnetic/ferroelectric composites has been extensively discussed due to their low energy consumption,[20–24] while many issues are still waiting to be solved for real applications. For instance, the strain-mediated magnetoelectric (ME) heterostructures have high operation voltage, substrate clamping effect, hard-to-integrate issues.[25,26] Meanwhile, the interfacial charge-mediated ME effect is relatively slow and corrosive, limiting their applications to integrated circuit chips (ICs) [27].

Light is essentially electromagnetic waves; therefore, controlling spins directly by light is the dream goal of researchers. Moreover, solar energy is renewable, completely clean, environmentally friendly, and abundant in nature. Efficiently utilizing solar power is crucial for the energy crisis. For example, sunlight controllable spintronics may be candidates for future spintronics because of their energy-efficient advantage and other benefits. Nowadays, laser or

* Corresponding authors.
** Corresponding author at: National Synchrotron Radiation Laboratory, University of Science and Technology of China, Hefei, 230029, Anhui, China.
E-mail addresses: wanglei.icer@xjtu.edu.cn (L. Wang), liqian89@ustc.edu.cn (Q. Li), ziyaozhou@xjtu.edu.cn (Z. Zhou).
[1] These authors contributed equally to this work.

https://doi.org/10.1016/j.nantod.2022.101605
1748-0132/

polarized light control of spins is investigated [28–38], while light-spin coupling efficiency is still low due to the intrinsic frequency mismatch between spin and laser light. We recently developed a sunlight control of interfacial magnetism in optical-magneto-electric tri-coupled ferromagnetic/photovoltaic heterostructure.[39] Magnetism is effectively manipulated by regulating the d orbital and introducing photoelectrons. Further on, enhancing the sunlight tunability and create non-volatility of photovoltaic/ferromagnetic heterostructures is substantial for real sunlight-driven spintronic devices, particularly memories.

This work fabricated ferromagnetic (CoFeB, 1.5 nm)/interlayer/photovoltaic (p-n junction Si) heterostructures. We inserted an interlayer (Ta, Cu) between ferromagnetic and photovoltaic layers to study the behavior of sunlight controlling interfacial magnetism. Under 1.4 sunlight intensities of illumination, the saturation magnetization (M_s) was reduced by 8.3 % and 7.6 % in the Ta inserted heterostructure and the Cu inserted heterostructure, respectively. In Cu inserted heterostructure, the M_s can be tuned reversibly with enhanced tunability. More interestingly, the M_s did not return to its initial position after closing the sunlight in Ta inserted heterostructure, indicating an apparent non-volatile behavior. The first-principles calculation was conducted to reveal the photo-induced electron movement and corresponding ferromagnetic changes during sunlight illumination. The Cu promoted the photoelectron transmission toward the CoFeB layer, leading to a larger M_s tunability due to more d orbital occupation in Cu inserted heterostructures. Meanwhile, the Ta also promoted photoelectron transmission and generated a potential barrier at the CoFeB/Ta interface to keep some photoelectrons in the CoFeB layer, creating a non-volatile magnetization switching. We then applied a small voltage (1 mV) on the Ta/CoFeB layer. The M_s was restored to its initial position, confirming our calculation and leading to switching from sunlight/electric dual-controllable tri-state magnetization. In addition, Element-resolved X-ray circular dichroism (XMCD) measurement was carried out to prove the change of intrinsic magnetism and the non-volatility during sunlight illumination. Our finding provides an alternative method of sunlight control of magnetism with non-volatility and paves a way toward energy-efficient sunlight tunable non-volatile spintronics devices like memories.

Results and discussion

The schematic of the photovoltaic spintronic heterostructure is shown in Fig. 1a. The p-n Si substrate is utilized as a visible light respond layer to generate the photo-induced electrons according to our previous work,[44] on which two different interlayered (Cu, Ta) (2 nm)/CoFeB (1.5 nm)/(Ta, Cu) (2 nm) heterostructures were deposited. And *I-V* curves of p-n Si and p-n Si/Ta(or Cu)/CoFeB are also available respectively in Fig. S14 to evidence the generation of photo-induced electrons. The cross-section image of heterojunction is shown in Fig. 1b, showing clear boundaries of each layer. Figs. 1c and 1d summarize the sunlight-induced M_s changes of Cu and Ta inserted heterostructures, respectively. In Cu-inserted heterostructure, the M_s decreased from 1691 emu cm^{-3} to 1647 emu cm^{-3} and 1562 emu cm^{-3} under 60 mW cm^{-2} (0.6 sun) and 140 mW cm^{-2} (1.4 sun) sunlight illumination, correspondingly. In Ta-inserted heterostructure, the M_s decreased from 1680 emu cm^{-3} to 1590 emu cm^{-3} and 1540 emu cm^{-3} with 0.6 sun and 1.4 sun illumination, accordingly. Our results show that the photo-induced electrons (PIEs) are excited in the p-n junction, transferred to the magnetic layer (CoFeB), filling D-orbits and leading to the magnetism change [39].

Here, we define the M_s change ratio as $\Delta M_s = (M_{s,dark} - M_{s,illumination}) / M_{s,dark}$. In Fig. 1e, the ΔM_s of Cu-inserted heterostructure decreases by 2.6 % and 7.6 % under 0.6 sun and 1.4 sun illumination, respectively. Compared with our previous results, the M_s regulation is significantly enhanced due to the more absorbed photon [39] The increase of M_s tunability was also realized in Ta-inserted one, where 0.6 and 1.4 sun illumination induced 5.3 % and 8.3 % ΔM_s. We also confirm the M_s variation of similar heterostructures is negligible on ordinary Si without p-n junction, excluding the thermal effect (Fig. S1 in Supporting Information). The ferromagnetic resonance shifts of Cu and Ta inserted samples under sunlight illumination were measured by electron spin-resonance (ESR) method and summarized in Fig. S3, confirming the M_s change from another respective. Interestingly, sunlight control of magnetism of Cu-inserted heterostructure has good reversibility (Fig. 1e). However, the M_s switching of the Ta-inserted sample is non-volatile; in other words, the M_s did not restore to its initial state after sunlight illumination, as shown in Fig. 1f. For sunlight-driven spintronics devices, non-volatility is crucial in data storage, enabling low-power consumption and the efficient use of sunlight.

Figs. 2 and 3 show the sunlight-induced M_s switching of the Cu-inserted and Ta-inserted heterostructure, respectively. An external magnetic field at 1 T was applied to stabilize the M_s in both cases. Then, the relationship between magnetization and time (M-T) is carried out under different sunlight illumination sequences, as shown in Figs. 2a, 3a. Firstly, we tested the stability of M_s in Cu-inserted heterostructure under various sunlight illumination, confirming that the photovoltaic effect is stable for the M-T investigation. In addition, the M_s was switched back and forth with the 1.4 sun illumination turned on and off, generating a sunlight controllable magnetic bi-state switching and enabling a “0” and “1” data bit for future sunlight tunable memories. Fig. 2c discusses the detailed photovoltaic control of the interfacial magnetism process. The unexcited electrons are distributed in the p-n Si substrate at the initial state (dark). When the p-n junction is in light soaking, the photos could be absorbed and generated by electron-hole pairs (EHPs). Then the EHPs are immediately separated as the electrons and holes. The photoelectrons flow into the n region and then migrated to the CoFeB layer through Cu under the p-n junction driving force (State I). At state II, the driving force of carrier migration disappears after the light is turned off, making the electrons and holes recombine and quench.

Nevertheless, full reversibility is not good enough for photovoltaic spintronic devices, particularly memories with non-volatility. To establish non-volatility, we need to keep the generated photoelectrons within the magnetic layer, maintaining the M_s change after sunlight illumination. One promising way is to create a potential barrier between the ferromagnetic layer and the p-n Si, preventing the photoelectrons from returning to p-n Si and recombine with holes after light illumination. Here, in Ta inserted heterostructures, the M-T switching curves were also measured, showing good stability and two magnetic states (light and dark) with and without sunlight in Fig. 3a, respectively. Unlike the Cu inserted ones, the M_s did not return to the dark state after sunlight illumination, creating a third state with M_s value between dark and light states. We then applied a small voltage (1 mV), the M_s returns to its initial position, proving our hypothesis that the photoelectrons can be stored in the ferromagnetic layer and manipulated by an external electric field. Fig. 3c represents the three states of Ta inserted heterostructure. At state I, the photoelectrons migrated to the CoFeB layer through Ta under the p-n junction driving force, similar to the state I of Cu inserted heterostructures. At state II without light illumination, the driving force disappears, allowing some electrons to recombine with holes. Unlike the Cu layer case, there are still many photoelectrons that stay in the CoFeB layer. In-state III, the external voltage drives the remaining electrons to move back to the p-n Si, and the M_s value restores to state I. In short, we realized a magnetic tri-states switching that can be controlled by both optical- and electric fields. Similarly, the obvious non-volatility in p-n Si/Ta/CoFeB/Cu and nice reversibility in p-n Si/Cu/CoFeB/Ta by measuring resistance are observed in Fig. S13, and

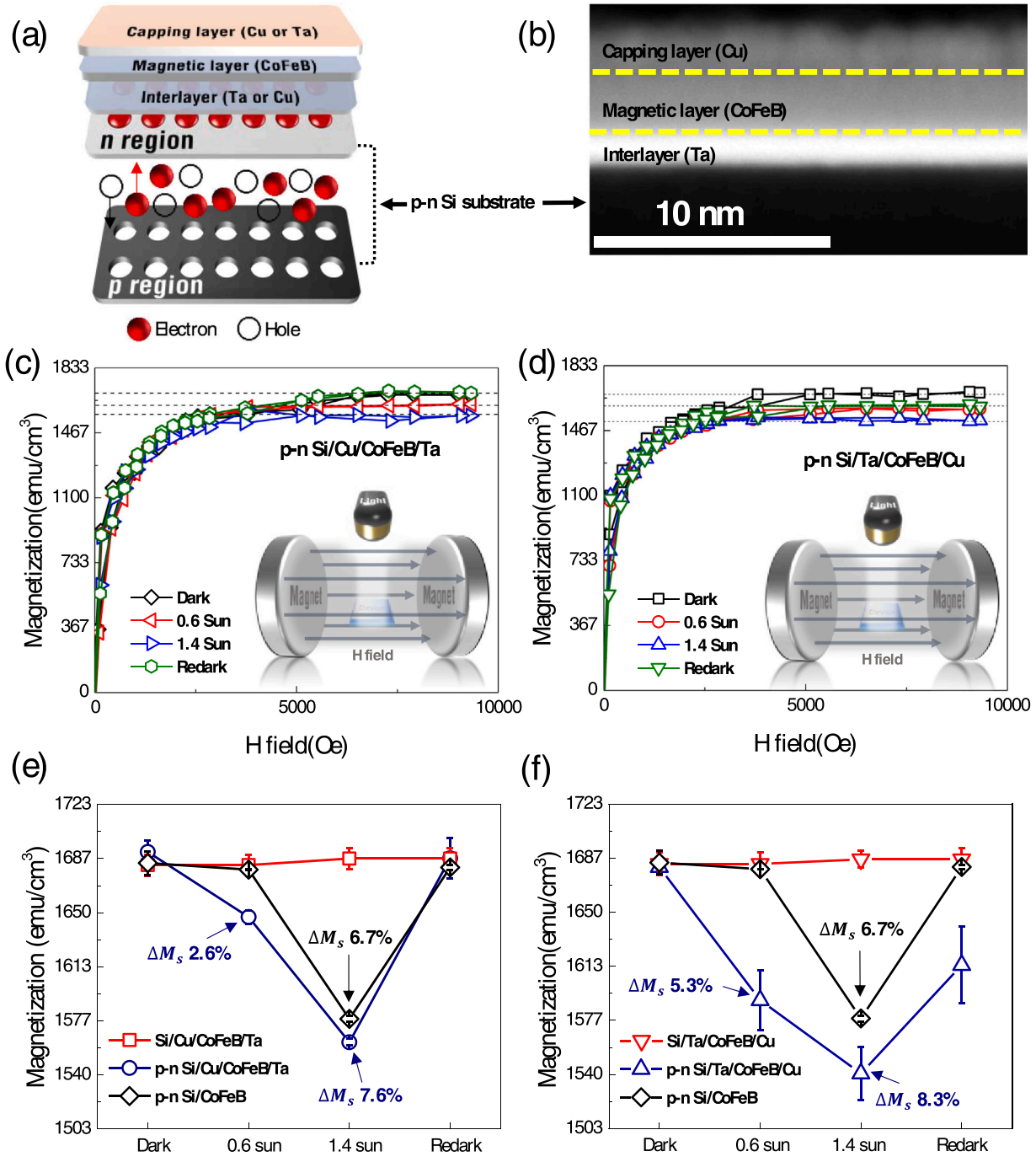

Fig. 1. Schematic diagram of structure and change of M_S. (a) Heterojunction structure schematics of photovoltaic spintronic devices. (b) The TEM images of photovoltaic heterojunction structure. (c) VSM of Cu-inserted heterostructure with different conditions. (Dark, 0.6 sun illumination, 1.4 sun illumination and After illumination) (d) VSM of Ta-inserted heterostructure with different conditions. (Dark, 0.6 sun, 1.4 sun and After illumination) (e) M_S of p-n Si/Cu/CoFeB/Ta, p-n Si/CoFeB and Si/Cu/CoFeB/Ta with different conditions, respectively. (Dark, 0.6 sun, 1.4 sun and After illumination) (f) M_S of p-n Si/Ta/CoFeB/Cu, p-n Si/CoFeB and Si/Ta/CoFeB/Cu with different conditions, respectively. (Dark, 0.6 sun, 1.4 sun, and After illumination).

it is evident that inserted Ta layer can block the parts of electrons back with light off. On the other hand, we can see that the resistance changes of p-n Si/Ta/CoFeB/Cu and p-n Si/Cu/CoFeB/Ta by thermal effect can be almost ignored compared with the changes under light illumination. It suggests that the resistance shifts of p-n Si/Ta/CoFeB/Cu and p-n Si/Cu/CoFeB/Ta primarily attributes to the injection of PIEs under light illumination. And it is consistent with our control experiments on Si/Ta/CoFeB/Cu and Si/Cu/CoFeB/Ta in VSM method. Therefore, the method of measuring resistance is another strong evidence for illustrating the non-volatility for memory application by inserting the Ta film to be the buffer layer between photovoltaic film (p-n Si wafer) and ferromagnetic film (CoFeB).

Element-resolved X-ray magnetic circular dichroism (XMCD) measurement was performed to reveal the change of intrinsic magnetism with sun illumination. The X-ray absorption spectra (XAS) at the Co edge were measured with the sample at normal incidence of circular x-ray and CoFeB magnetization aligned parallel or antiparallel to the incidence direction of x-ray, as shown in Fig. 4(a). Fig. 4(c)-(e) show the XMCD intensity at Co L_3 edge decreases from ~11.5 % to ~5.4 % after sun illumination and stabilizes at ~4.1 % after removing the sun illumination, while the XMCD

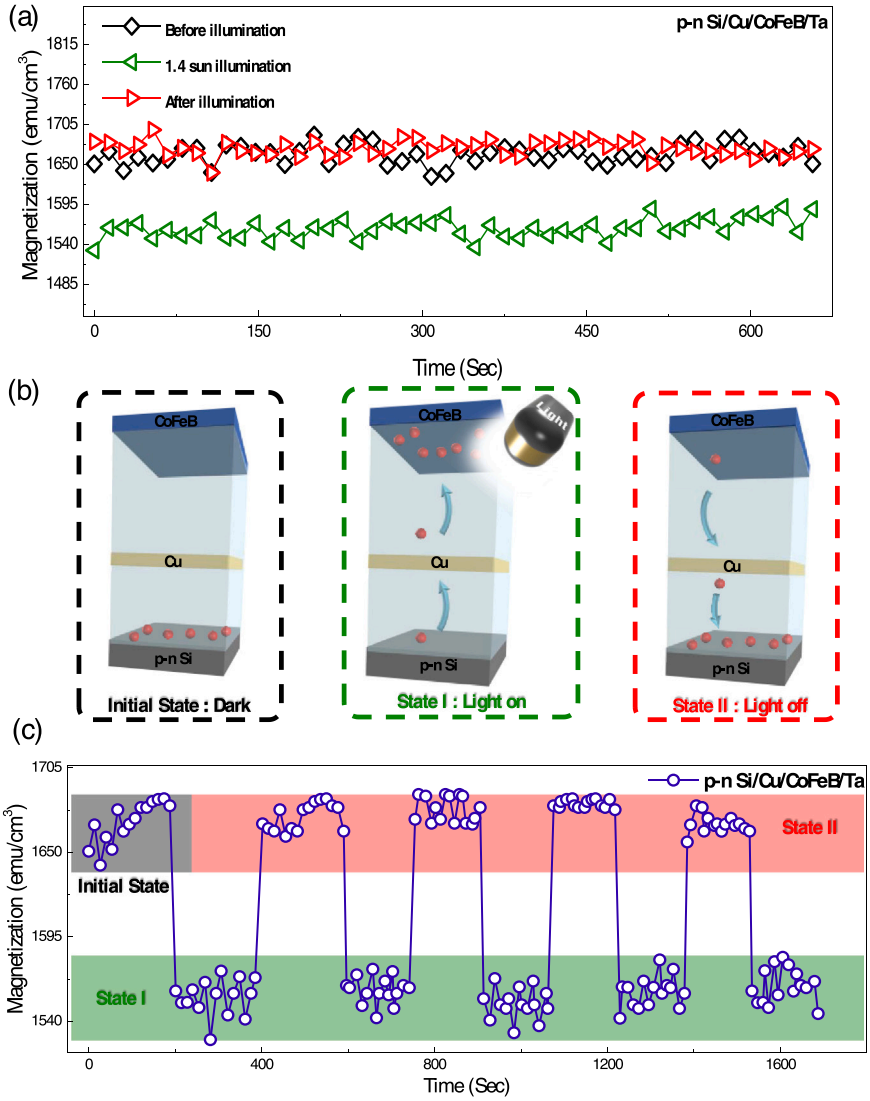

Fig. 2. Stability, mechanism diagram and cycling characteristic of p-n Si/Cu/CoFeB/Ta structure. (a) Stability in magnetization – Time (M-T) test of Cu-inserted heterostructure under magnetic field (H-field) 10,000 Oe by VSM under different conditions. (b) The mechanism diagram of Initial State, State I, and State II represents Cu-inserted heterostructure before, during, and after light illumination, respectively. (c) Cycling characteristic of the M-T in the photovoltaic control of Cu-inserted heterostructure with Initial State, State I, and State II, respectively.

intensity at Co L_2 edge changes from ~3.6 % to ~5.0 % after sun illumination, and stabilizes at ~3.0 % after removing the sun illumination. The obvious drop of XMCD intensity at Co L_3 edge suggests the decrease of magnetism after sun illumination and the non-volatile change of magnetism after removal of illumination in the CoFeB layer. The slight increase of XMCD intensity at Co L_2 edge after sun illumination suggests the redistribution of the orbital moment and spin moment to CoFeB magnetization. According to the sum rule,[40] the orbital and spin magnetic moments can be determined after considering the ~50 % degree of circular x-ray polarization and 7.51 for electron occupation number of Co. The spin moment dropped from 0.514 μ_B/atom to 0.456 μ_B/atom after sun illumination and 0.232 μ_B/atom without illumination, while the orbital moment dropped from 0.097 μ_B/atom to almost zero ~0.003 μ_B/atom after sun illumination and 0.0065 μ_B/atom without illumination. The result further demonstrates the non-volatile control of magnetism with sun illumination. In addition, X-ray circular XMCD dichroism measurement in hetero-structure of p-n Si/Cu/CoFeB/Ta is shown in Fig. S12, suggesting the magnetism of CoFeB could recover to its unilluminated state.

The external charge could change the magnetism significantly in conventional ferromagnetic materials [39,41–43]. It is not surprising that the photoelectrons induced by the illumination on p-n Si can get into the magnetic layer and decrease the magnetic moments in the CoFeB, accordingly. However, from the above discussion, the inserting layers of Cu and Ta show quite a different feature on the behavior of the reproducible tests, where inserting Ta changes the magnetic moments of the CoFeB layer non-volatilely when turning off the sunlight. The first principle calculations are carried out using the VASP package to reveal the underlying physics of the above phenomenon qualitatively. The inserting Ta or Cu layers are the keys, and the magnetic layer should be less important, so we use CoFe instead of CoFeB for simplicity.

We first set up Ta/CoFe and Cu/CoFe multilayers as shown in Fig. 5(a1) and (a2), respectively, and calculate their corresponding charge density n_e at equilibrium state. After that, 100 extra electrons are introduced into the system to simulate the photoelectrons from p-n Si, therefore the charge density under sunlight n_{ph} can be obtained accordingly. In this way, charge density difference $\Delta n = n_{ph} - n_e$ will show the location of photoelectrons. Fig. 5(b1) and (b2) plot the typical sections of the corresponding distributions

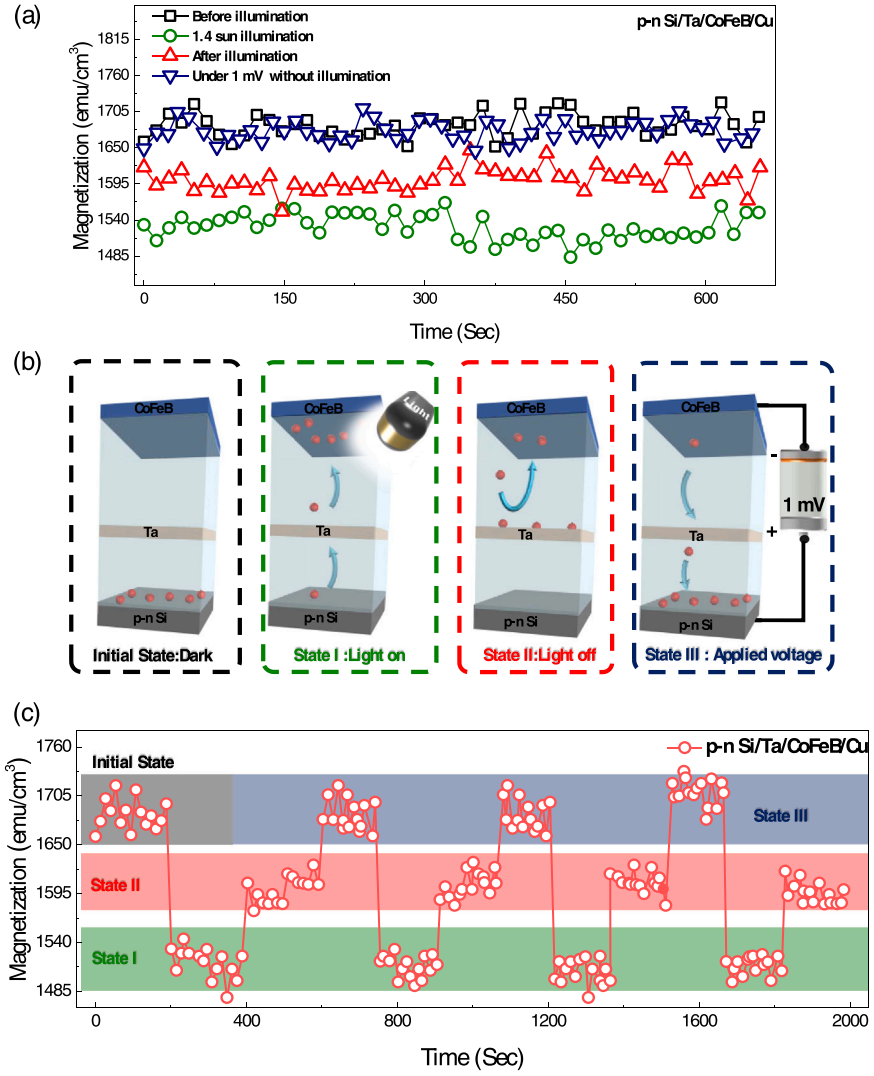

Fig. 3. Stability, mechanism diagram and cycling characteristic of p-n Si/Ta/CoFeB/Cu structure. (a) Stability in magnetization – Time (M-T) test of Ta-inserted heterostructure under magnetic field (H field) 10,000 Oe by VSM under different conditions. (b) Themechanism diagram of Initial State, State I, State II, and State III represents the Ta-inserted heterostructure before light illumination, during the light illumination, after light illumination, an applied voltage of 1 mV, respectively. (c) Cycling characteristic of the M-T in the photovoltaic control of Ta-inserted heterostructure with Initial State, State I, State II, and State III, respectively.

of Δn in the whole system. The photoelectrons are mainly localized around Co or Fe atoms in Ta/CoFe, but more free electrons are distributed at the Cu side (broadened yellow color) in Cu/CoFe. On top of the above results, we can conclude that the Ta is more "photoelectron repellent" than Cu when constructing magnetic multilayers with CoFe. This can be understood by the energy levels of the corresponding atoms. If the electrons diffuse to the magnetic multilayers, we know that they will first try to fill the unoccupied bands of the system: the localized 5d of Ta, 3d of CoFe, and the free 4 s of Cu, as shown in Fig. 5(c). When the p-n Si/Ta/CoFe/Cu and p-n Si/Cu/CoFe/Ta hetero-structures are in the light soaking, respectively, the p-n Si wafer can be excited to generate the PIEs. The PIEs are then injected into CoFeB for charge separation through the inserted layer (Ta or Cu) under enough driving force. It comes from the built-in electric field, which originated from the potential difference between n region and p region under constant illumination. In both Ta/CoFeB and Cu/CoFeB, the energy barrier of 4 s in Cu and 5d in Ta can be overcome to make the PIEs transfer. The M_s of CoFeB is finally depressed under illumination due to that the 3d band of CoFeB is occupied by PIEs. It is consistent with our previous work.[44] When turning off the sunlight, the recombination of PIEs is dominated, and there is not enough driving force. However, the PIEs will be partially blocked due to the higher energy level of the 5d band of Ta. In this sense, the remaining PIEs inside the CoFeB layer still depress the corresponding M_s, and the non-volatile behavior of M_s is then achieved in p-n Si/Ta/CoFeB/Cu hetero-structures when turning off the sunlight Similarly, the sample used Ru with 4d, and 5 s orbitals as the interlayer in p-n Si/Ru/CoFeB/Cu heterojunction was also investigated. As shown in Fig. S6, 17.8 % of magnetization variation is observed under 1.4 sun illumination, and it also exhibits the same non-volatile behavior after illumination. These Ru results provide additional proof of our theoretical explanation to support our experimental phenomenon, making the photoelectrons hold much longer time in CoFe and thus end up with the non-volatile behavior of the photovoltaic spintronics device by inserting Ta layer with the higher energy level of orbitals.

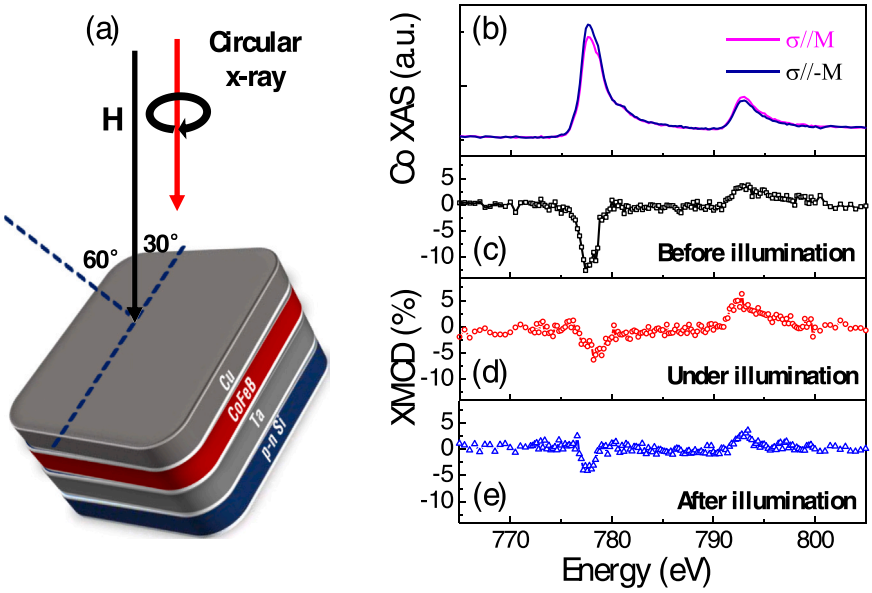

Fig. 4. X-ray magnetic circular dichroism (XMCD) measurement. (a) Schematic drawing of the X-ray magnetic circular dichroism (XMCD) measurement. (b) X-ray absorption spectra (XAS) at Co edge from CoFeB at normal incidence of X-ray. The pink and navy lines represent the XAS with magnetization parallel and antiparallel to the circular x-ray, respectively. The XMCD of CoFeB (c) before illumination, (d) with sun illumination, and (e) after removal of sun illumination.

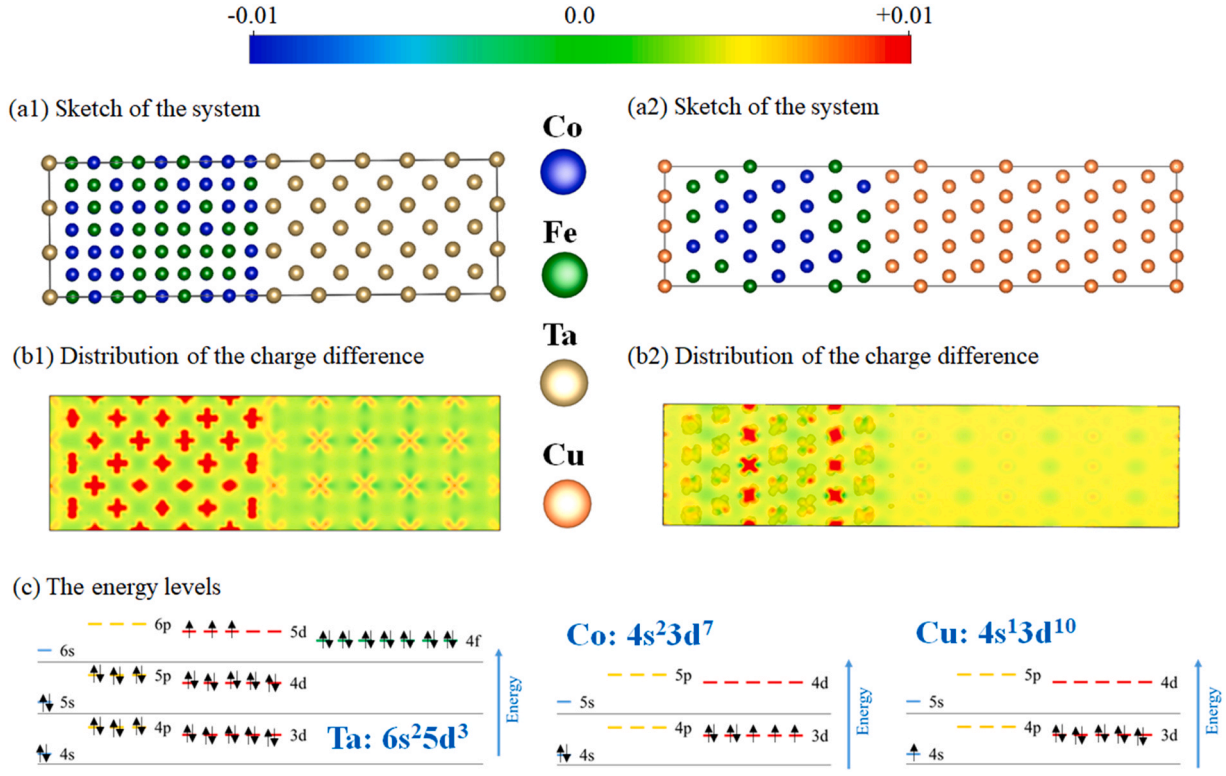

Fig. 5. First-principles calculations for non-volatile engineering. The calculated charge density difference $\Delta n = n_{ph} - n_e$, where, n_e is the charge density of the equilibrium state and n_{ph} represents the charge density when introducing photoelectrons. (a1) and (a2) illustrate the sketch model of the calculated systems of Ta=CoFe, and Cu=CoFe multilayers, respectively. (b1) and (b2) are the distributions of Δn of the typical sections with the color bar above. (c) shows the energy levels of the elements in the system, accordingly. Here, Fe is omitted as it is only one electron different from Co.

Conclusion

In summary, the photovoltaic heterostructures of p-n Si/Cu/CoFeB/Ta and p-n Si/Ta/CoFeB/Cu were studied in our experiment. The saturated magnetization of Cu and Ta inserted heterojunctions are tuned by 7.6 % and 8.3 % under 1.4 sun illumination, respectively. The Cu inserted heterojunction exhibits good reversibility, while the Ta inserted heterojunction creates a non-volatility. The first-principles calculations reveal that both Cu and Ta layers promote photoelectron transmission and enhance optical-magneto-electric tunability. Most importantly, the Ta creates a potential barrier at the Ta/CoFeB interface to block the photoelectrons and generates a

sunlight/electric dual controllable magnetic tri-state, which may open a door towards low-power, sunlight-driven spintronics devices with non-volatile memory functionality.

Experimental section

Fabrication and characterization of the photovoltaic spintronic device

The device diagram of photovoltaic spintronics is p-n Si/Cu (2 nm)/$Co_{40}Fe_{40}B_{20}$ (1.5 nm)/Ta (2 nm) and p-n Si/Ta (2 nm)/$Co_{40}Fe_{40}B_{20}$ (1.5 nm)/Cu (2 nm). The Ta, Cu, and CoFeB films were all deposited by a DC magnetron sputtering under vacuum (9×10^{-8} Torr) at room temperature. The film thickness was controlled with quartz crystal microbalance integrated into the magnetron sputtering system in the coating process. No further in situ annealing was carried out. The Si wafers with p-n junction were purchased from Shunsheng electronic technology co. LTD (China) and used as photo absorption media. The epitaxial n type layer (thickness of 10 μm, resistance < 0.02 Ω cm) is fabricated onto the p type Si substrate (thickness of 525 μm, resistance of 4–5 Ω cm) to form the p-n junction Si wafer.

The in situ measurement of magnetic properties

In situ magnetic anisotropy modification was carried out in VSM (Lakeshore 7404) and in the ESR spectra (JES-FA200, JEOL RESONANCE Inc.), the rotator of which can show the angle between the film plane and the applied magnetic field. The TE 011 mode microwave power by the microwave unit was 9200 MHz. Devices were illuminated under AM 1.5 G (100 mW cm^{-2}) using a PL-XQ500W Xenon lamp solar simulator. The standard intensity of sunlight illumination is 100 mW cm^{-2} (1 sun).

X-ray magnetic circular dichroism (XMCD) measurement

The XMCD measurement was conducted at the "XMCD-a" beamline of the National Synchrotron Radiation Laboratory (NSRL) in China. The intensity of X-ray absorption spectra was recorded in total electron yield. In the XMCD measurement, we applied a magnetic field of 1000 Oe along the normal direction of the sample, which is large enough to saturate the magnetization of the CoFeB layer.

Declaration of Competing Interest

The authors declare that they have no known competing financial interests or personal relationships that could have appeared to influence the work reported in this paper.

Acknowledgments

Y.Z. and Y.D. contributed equally to this work. The work was supported by the National Natural Science Foundation of China (Grant Nos. 52172126, 91964109, 11534015, 51802248, 62001366, 11804266, 12174364), the National Key R&D Program of China (2019YFA0307900, 2018YFB0407601), the National 111 Project of China (B14040), the China Postdoctoral Science Foundation (Grant Nos. 2021T140549). The authors acknowledge the support from the International Joint Laboratory for Micro/Nano Manufacturing and Measurement Technologies and the support by the Users with Excellence Program of Hefei Science Center CAS (No. 2021HSC-UE003).

Author Statement

This submitted revised manuscript of "*Sunlight-Induced Tri-State Spin Memory in Photovoltaic/Ferromagnetic Heterostructure*" has been certified and approved by the all authors. The article of "*Sunlight-Induced Tri-State Spin Memory in Photovoltaic/Ferromagnetic Heterostructure*" is our original work and we guarantee that this work hasn't received prior publication and isn't under consideration for publication elsewhere as well.

Appendix A. Supporting information

Supplementary data associated with this article can be found in the online version at doi:10.1016/j.nantod.2022.101605.

References

[1] A. Brataas, A.D. Kent, H. Ohno, Current-induced torques in magnetic materials, Nat. Mater. 5 (2012) 372–381.
[2] T. Jungwirth, X. Marti, P. Wadley, J. Wunderlich, Antiferromagnetic spintronics, Nat. Nanotechnol. 3 (2016) 231–241.
[3] A. Avsar, J.Y. Tan, M. Kurpas, M. Gmitra, K. Watanabe, T. Taniguchi, J. Fabian, B. Özyilmaz, Gate-tunable black phosphorus spin valve with nanosecond spin lifetimes, Nat. Phys. 9 (2017) 888–893.
[4] C. Song, Y. You, X. Chen, X. Zhou, Y. Wang, F. Pan, How to manipulate magnetic states of antiferromagnets, Nanotechnology 11 (2018) 112001.
[5] K. Zhai, D.S. Shang, Y.S. Chai, G. Li, J.W. Cai, B.G. Shen, Y. Sun, Room-temperature nonvolatile memory based on a single-phase multiferroic hexaferrite, Adv. Funct. Mater. 9 (2018) 1705771.
[6] X.F. Zhou, J. Zhang, F. Li, X.Z. Chen, G.Y. Shi, Y.Z. Tan, Y.D. Gu, M.S. Saleem, H.Q. Wu, F. Pan, C. Song, Strong orientation-dependent spin-orbit torque in thin films of the antiferromagnet Mn2Au, Phys. Rev. Appl. 5 (2018) 054028.
[7] Y. Sun, X. Zhao, C. Song, K. Xu, Y. Xi, J. Yin, Z. Wang, X. Zhou, X. Chen, G. Shi, H. Lv, Q. Liu, F. Zeng, X. Zhong, H. Wu, M. Liu, F. Pan, Performance-enhancing selector via symmetrical multilayer design, Adv. Funct. Mater. 13 (2019) 1808376.
[8] A.J. Tan, M. Huang, C.O. Avci, F. Buttner, M. Mann, W. Hu, C. Mazzoli, S. Wilkins, H.L. Tuller, G.S.D. Beach, Magneto-ionic control of magnetism using a solid-state proton pump, Nat. Mater. 1 (2019) 35-+.
[9] L. Zhang, J. Chen, X. Zheng, B. Wang, L. Zhang, L. Xiao, S. Jia, Gate-tunable large spin polarization in a few-layer black phosphorus-based spintronic device, Nanoscale 24 (2019) 11872–11878.
[10] V.I. Nizhankovskii, L.B. Lugansky, Vibrating sample magnetometer with a step motor, Meas. Sci. Technol. 5 (2007) 1533–1537.
[11] J.A. Weil, A review of electron spin spectroscopy and its application to the study of paramagnetic defects in crystalline quartz, Phys. Chem. Miner. 4 (1984) 149–165.
[12] R.P. Guertin, S. Foner, Application of a vibrating sample magnetometer to magnetic measurements under hydrostatic pressure, Rev. Sci. Instrum. 6 (1974) 863–864.
[13] S. Foner, Versatile and sensitive vibrating-sample magnetometer, Rev. Sci. Instrum. 7 (1959) 548–557.
[14] M. Tsoi, A.G.M. Jansen, J. Bass, W.C. Chiang, M. Seck, V. Tsoi, P. Wyder, Excitation of a magnetic multilayer by an electric current, Phys. Rev. Lett. 19 (1998) 4281–4284.
[15] E.B. Myers, D.C. Ralph, J.A. Katine, R.N. Louie, R.A. Buhrman, Current-induced switching of domains in magnetic multilayer devices, Science 5429 (1999) 867–870.
[16] J.A. Katine, F.J. Albert, R.A. Buhrman, E.B. Myers, D.C. Ralph, Current-driven magnetization reversal and spin-wave excitations in Co/Cu/Co pillars, Phys. Rev. Lett. 14 (2000) 3149–3152.
[17] V.S. Pribiag, I.N. Krivorotov, G.D. Fuchs, P.M. Braganca, O. Ozatay, J.C. Sankey, D.C. Ralph, R.A. Buhrman, Magnetic vortex oscillator driven by d.c. spin-polarized current, Nat. Phys. 7 (2007) 498–503.
[18] C.C. Chiang, S.Y. Huang, D. Qu, P.H. Wu, C.L. Chien, Absence of evidence of electrical switching of the antiferromagnetic neel vector, Phys. Rev. Lett. 22 (2019) 227203.
[19] G.D.H. Wong, W.C. Law, F.N. Tan, W.L. Gan, C.C.I. Ang, Z. Xu, C.S. Seet, W.S. Lew, Thermal behavior of spin-current generation in PtxCu1-x devices characterized through spin-torque ferromagnetic resonance, Sci. Rep. (2020) 1.
[20] S. Zhao, Z. Zhou, C. Li, B. Peng, Z. Hu, M. Liu, Low-voltage control of (Co/Pt) x perpendicular magnetic anisotropy heterostructure for flexible spintronics, ACS Nano 7 (2018) 7167–7173.
[21] C. Song, B. Cui, F. Li, X. Zhou, F. Pan, Recent progress in voltage control of magnetism: materials, mechanisms, and performance, Prog. Mater. Sci. (2017) 33–82.
[22] B. Peng, Z. Zhou, T. Nan, G. Dong, M. Feng, Q. Yang, X. Wang, S. Zhao, D. Xian, Z.D. Jiang, W. Ren, Z.G. Ye, N.X. Sun, M. Liu, Deterministic switching of perpendicular magnetic anisotropy by voltage control of spin reorientation transition in (Co/Pt)3/Pb(Mg1/3Nb2/3)O3-PbTiO3 multiferroic heterostructures, ACS Nano 4 (2017) 4337–4345.
[23] M. Liu, Z. Zhou, T. Nan, B.M. Howe, G.J. Brown, N.X. Sun, Voltage tuning of ferromagnetic resonance with bistable magnetization switching in energy-efficient magnetoelectric composites, Adv. Mater. 10 (2013) 1435–1439.

[24] M. Liu, B.M. Howe, L. Grazulis, K. Mahalingam, T. Nan, N.X. Sun, G.J. Brown, Voltage-impulse-induced non-volatile ferroelastic switching of ferromagnetic resonance for reconfigurable magnetoelectric microwave devices, Adv. Mater. 35 (2013) 4886–4892.
[25] M. Zhu, Z. Zhou, B. Peng, S. Zhao, Y. Zhang, G. Niu, W. Ren, Z.-G. Ye, Y. Liu, M. Liu, Modulation of spin dynamics via voltage control of spin-lattice coupling in multiferroics, Adv. Funct. Mater. 10 (2017) 1605598.
[26] X. Xue, Z. Zhou, G. Dong, M. Feng, Y. Zhang, S. Zhao, Z. Hu, W. Ren, Z.G. Ye, Y. Liu, M. Liu, Discovery of enhanced magnetoelectric coupling through electric field control of two-magnon scattering within distorted nanostructures, ACS Nano 9 (2017) 9286–9293.
[27] Q. Yang, Z. Zhou, L. Wang, H. Zhang, Y. Cheng, Z. Hu, B. Peng, M. Liu, Ionic gel modulation of RKKY interactions in synthetic anti-ferromagnetic nanostructures for low power wearable spintronic devices, Adv. Mater. 22 (2018) 1800449.
[28] F. Willems, C. von Korff Schmising, C. Struber, D. Schick, D.W. Engel, J.K. Dewhurst, P. Elliott, S. Sharma, S. Eisebitt, Optical inter-site spin transfer probed by energy and spin-resolved transient absorption spectroscopy, Nat. Commun. 1 (2020) 871.
[29] P. Tengdin, C. Gentry, A. Blonsky, D. Zusin, M. Gerrity, L. Hellbruck, M. Hofherr, J. Shaw, Y. Kvashnin, E.K. Delczeg-Czirjak, M. Arora, H. Nembach, T.J. Silva, S. Mathias, M. Aeschlimann, H.C. Kapteyn, D. Thonig, K. Koumpouras, O. Eriksson, M.M. Murnane, Direct light-induced spin transfer between different elements in a spintronic Heusler material via femtosecond laser excitation, Sci. Adv. 3 (2020) eaaz1100.
[30] J. He, T. Frauenheim, Optically driven ultrafast magnetic order transitions in two-dimensional ferrimagnetic MXenes, J. Phys. Chem. Lett. 15 (2020) 6219–6226.
[31] F. Siegrist, J.A. Gessner, M. Ossiander, C. Denker, Y.P. Chang, M.C. Schroder, A. Guggenmos, Y. Cui, J. Walowski, U. Martens, J.K. Dewhurst, U. Kleineberg, M. Munzenberg, S. Sharma, M. Schultze, Light-wave dynamic control of magnetism, Nature 7764 (2019) 240–244.
[32] C.H. Lambert, S. Mangin, B. Varaprasad, Y.K. Takahashi, M. Hehn, M. Cinchetti, G. Malinowski, K. Hono, Y. Fainman, M. Aeschlimann, E.E. Fullerton, All-optical control of ferromagnetic thin films and nanostructures, Science 6202 (2014) 1337–1340.
[33] A.V. Kimel, M. Li, Writing magnetic memory with ultrashort light pulses, Nat. Rev. Mater. 3 (2019) 189–200.
[34] S. Iihama, Y. Xu, M. Deb, G. Malinowski, M. Hehn, J. Gorchon, E.E. Fullerton, S. Mangin, Single-shot multi-level all-optical magnetization switching mediated by spin transport, Adv. Mater. 51 (2018) e1804004.
[35] M. Deb, M. Vomir, J.L. Rehspringer, J.Y. Bigot, Ultrafast optical control of magnetization dynamics in polycrystalline bismuth doped iron garnet thin films, Appl. Phys. Lett. 25 (2015) 252404.
[36] A. Kirilyuk, A.V. Kimel, T. Rasing, Laser-induced magnetization dynamics and reversal in ferrimagnetic alloys, Rep. Prog. Phys. 2 (2013) 026501.
[37] A. Kirilyuk, A.V. Kimel, T. Rasing, Controlling spins with light, Philos. Trans. A Math. Phys. Eng. Sci. 1951 (2011) 3631–3645.
[38] D. a Pejaković, A., C. Kitamura, J.S. Miller, A.J. Epstein, Optical control of magnetic order in molecule-based magnet Mn(TCNE)[sub x]·y(CH[sub 2]Cl[sub 2]), J. Appl. Phys. (2002) 10.
[39] Y. Zhao, S. Zhao, L. Wang, Z. Zhou, J. Liu, T. Min, B. Peng, Z. Hu, S. Jin, M. Liu, Sunlight control of interfacial magnetism for solar driven spintronic applications, Adv. Sci. 24 (2019) 1901994.
[40] C.T. Chen, Y.U. Idzerda, H. Lin, N.V. Smith, G. Meigs, E. Chaban, G.H. Ho, E. Pellegrin, F. Sette, Experimental confirmation of the X-ray magnetic circular dichroism sum rules for iron and cobalt, Phys. Rev. Lett. 1 (1995) 152–155.
[41] M. Guan, L. Wang, S. Zhao, Z. Zhou, G. Dong, W. Su, T. Min, J. Ma, Z. Hu, W. Ren, Z.-G. Ye, C.-W. Nan, M. Liu, Ionic modulation of the interfacial magnetism in a bilayer system comprising a heavy metal and a magnetic insulator for voltage-tunable spintronic devices, Adv. Mater. (2018) 40.
[42] M. Guan, L. Wang, S. Zhao, B. Peng, W. Su, Z. He, G. Dong, T. Min, J. Ma, Z. Hu, W. Ren, Z.-G. Ye, C.-W. Nan, Z. Zhou, M. Liu, Ionic modulation of interfacial magnetism in light metal/ferromagnetic insulator layered nanostructures, Adv. Funct. Mater. 1 (2019) 1805592.
[43] L. Wang, X.R. Wang, T. Min, K. Xia, Charge-induced ferromagnetic phase transition and anomalous Hall effect in full d-band nonmagnetic metals, Phys. Rev. B 22 (2019) 224416.
[44] Y. Zhao, S. Zhao, L. Wang, S. Wang, Y. Du, Y. Zhao, S. Jin, T. Min, B. Tian, Z. Jiang, Z. Zhou, M. Liu, Photovoltaic modulation of ferromagnetism within a FM metal/P-N junction Si heterostructure, Nanoscale 1 (2021) 272–279.